Chemical Physics Letters 610–611 (2014) 273–277

Contents lists available at ScienceDirect

Chemical Physics Letters

journal homepage: www.elsevier.com/locate/cplett

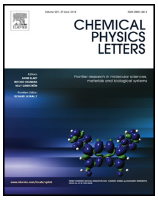

Analysis of hole transport in thin films and nanoparticle assemblies of poly(3-hexylthiophene)

Xu Han[a], Monojit Bag[b], Timothy S. Gehan[b], Dhandapani Venkataraman[b], Dimitrios Maroudas[a,*]

[a] Department of Chemical Engineering, University of Massachusetts, Amherst, MA 01003-9303, United States
[b] Department of Chemistry, University of Massachusetts, Amherst, MA 01003-9303, United States

ARTICLE INFO

Article history:
Received 17 June 2014
In final form 9 July 2014
Available online 28 July 2014

ABSTRACT

We report numerical simulation results on hole transport in layers of the organic polymer poly(3-hexylthiophene) (P3HT) of different nanostructures based on a deterministic, phenomenological drift–diffusion-reaction model that accounts for hole trapping–detrapping kinetics. The model is used to characterize the various P3HT layers examined in terms of their hole transport dispersivity. The model reproduces well experimental data of photocurrent evolution in P3HT samples ranging from drop cast thin films to surfactant-stabilized nanoparticle assemblies, explains the role of excess surfactant molecules in hole trapping for assemblies of P3HT nanoparticles, and demonstrates quantitatively the potential of using nanoparticle assemblies in organic photovoltaic devices.

1. Introduction

Recently, there has been a growing interest in using conjugated polymer nanoparticles [1] for the fabrication of organic active layers that are used in light-emitting diodes, organic solar cells, field-effect transistors, and other optoelectronic devices [2–4]. Using nanoparticles has the significant advantage that individual electron-donor and electron-acceptor particles of tunable size and internal structure can be pre-formed and then self-assembled into well-defined active-layer morphologies [5]. Moreover, using printing and coating methods, nanoparticles can be formulated as aqueous dispersions for large-area manufacturing making them attractive for active layer fabrication in organic photovoltaic cells. An important feature of conjugated polymer nanoparticles is that they are stabilized by surfactants, which are expected to introduce trapping sites for electrons and holes and impede charge transport. Yet, the observed hole mobility in surfactant-stabilized conjugated nanoparticle assemblies is comparable to that of pristine films [6]. In addition to charge mobility, charge trapping and detrapping also play an important role in the overall performance of these films as photovoltaic active layers. Herein, we address the questions of hole mobility and trapping through comparisons of the computed charge transport coefficients and trapping–detrapping kinetics in nanoparticle assemblies and pristine thin films of the electron-donor conjugated polymer poly(3-hexylthiophene) (P3HT) based on computer simulations of time-of-flight (TOF) experiments for measuring transient photocurrents in these P3HT layers.

Computational modeling is a powerful means to further our understanding of charge transport in organic polymer films. Dynamic Monte Carlo simulations have been used to understand mechanisms of charge carrier generation and transport [7,8]. Numerical simulations informed about such mechanisms have described satisfactorily physical properties of such organic layers [9]. Deterministic, phenomenological drift–diffusion-reaction models also have managed to capture transient photocurrents measured in bulk-heterojunction organic photovoltaic (OPV) devices [10–12]. The computational efficiency of such models, especially within the effective-medium approximation [12], is particularly appealing for the simulation of OPV device operation and the optimization of OPV device performance. Such deterministic models, however, have not been used to model charge transport in OPV active layers consisting of nanoparticle assemblies, where incorporating the kinetics of trapping and detrapping of charge carriers into the models is particularly important.

In this study, we examine hole transport dispersivity in thin films and nanoparticle assemblies of P3HT and explore the effects of surfactant on hole trapping. The purpose of this Letter is the development and validation of a deterministic, phenomenological drift–diffusion-reaction model for hole transport in P3HT thin

---

* Corresponding author.
E-mail address: maroudas@ecs.umass.edu (D. Maroudas).

http://dx.doi.org/10.1016/j.cplett.2014.07.022
0009-2614/

films and nanoparticle assemblies that can reproduce experimental data for photocurrent evolution in samples of these materials with different nanostructures and over a range of applied voltages. The model accounts for the kinetics of hole trapping and detrapping in the various P3HT films and is used to characterize the corresponding nanostructures in terms of their hole transport dispersivity, to explain the role of excess surfactant molecules in hole trapping for assemblies of P3HT nanoparticles, and to explore the potential of using nanoparticle assemblies as active layers in OPV devices.

2. Experimental methods, model, and computational methods

The experimental procedures followed for sample preparation and characterization and for the measurement of transient photocurrents were presented in Ref. [6]. P3HT thin films were drop cast on indium tin oxide (ITO) substrates. Some of the nanoparticle assemblies were prepared after centrifugal filtration of the dispersion in order to remove excess surfactant molecules. Both non-centrifuged and centrifuged nanoparticle assemblies were spray coated on the ITO substrates. A thin aluminum (Al) film was then thermally deposited on the P3HT layers. The Al electrode was positively biased with respect to the ITO electrode. 355-nm pulsed (~10 ns) laser illumination was applied near the Al electrode. The TOF method was used to determine hole mobilities [6]. Systematic experiments on various samples under different applied biases demonstrated hole mobility in assemblies of surfactant surrounded nanoparticles comparable with those of drop cast P3HT thin films. It was also found that the presence of excess surfactant in P3HT nanoparticle assemblies increased their hole transport dispersivity [6].

For a quantitative analysis of hole transport in the above three types of thin films and nanoparticle assemblies, we have developed a comprehensive one-dimensional (1D) transient drift–diffusion-reaction model. The model accounts for hole trapping and detrapping in addition to hole diffusion and drift and consists of coupled boundary-value problems (BVPs) for the evolution of the free and trapped hole density fields in the polymer layer and for the electrostatic potential distribution in the material, governed by the following equations:

$$\frac{\partial p_f}{\partial t} = \frac{1}{e}\frac{\partial}{\partial x}\left(\mu_p k_B T\frac{\partial p_f}{\partial x} - \mu_p p_f eE\right) - \frac{\partial p_t}{\partial t}, \tag{1}$$

$$\frac{\partial p_t}{\partial t} = C_t(P_t - p_t)p_f - C_{dt}p_t, \tag{2}$$

and

$$\frac{\partial^2 \Phi}{\partial x^2} = -\frac{e(p_f + p_t)}{\varepsilon_0 \varepsilon}. \tag{3}$$

Eq. (1) describes the evolution of the free hole density $p_f(x, t)$, where $p_t(x, t)$ is the trapped hole density. In Eq. (1), t, e, and x denote time, elementary charge, and the coordinate along the film thickness direction and perpendicular to the electrodes, respectively, k_B is Boltzmann's constant, T is temperature, and E is the magnitude of the electric field, $\mathbf{E} = E\mathbf{e}_x$, directed along x. The hole mobility, μ_p, is taken to follow the Poole–Frenkel relation [13], $\mu_p = \mu_0 \exp(\gamma|E|^{1/2})$, with μ_0 and γ being the zero-field mobility and the field dependence coefficient, respectively. For the free holes, boundary conditions of thermionic injection with image charge effects [14] were applied for the hole fluxes at the polymer/electrode interfaces, $x = 0$ and $x = L$. Eq. (2) expresses the kinetics of hole trapping and detrapping with the initial condition that no generated charges are trapped, $p_t(x, t = 0) = 0$; C_t and C_{dt} are the trapping and detrapping kinetic rate coefficients, respectively, and P_t is the density of trapping sites in the polymeric material. Trapping–detrapping kinetics according to Eq. (2) assumes a single trapping energy level. Eq. (3) is Poisson's equation for the electrostatic potential Φ, $E = -\partial\Phi/\partial x$, ε_0 is the vacuum permittivity and ε is the relative permittivity of the material; $p \equiv p_f + p_t$ is the total density of holes. Dirichlet boundary conditions for Φ were applied at $x = 0$ and $x = L$, as determined by the applied potentials at the two electrodes. As initial condition for the free hole density, we use an exponentially decaying (from $x = 0$) distribution, $p_f(x, 0) = P_0 \exp(-x/\lambda)$ [15], where λ is on the order of the penetration depth of the exciting light.

We solved the coupled BVPs governed by Eqs. (1)–(3) numerically using the finite-difference method for domain discretization. To avoid numerical instabilities in steep propagating charge fronts caused by strong electric fields, we employed upwinding [16] for the computation of the drift flux in Eq. (1). The convergence of the numerical results with refining the finite-difference grid resolution was ensured by using fine grids in the numerical simulations (with as many as $n = 6000$ grid points). We implemented the implicit Euler method for time stepping Eqs. (1) and (2) and calculated the transient photocurrent $I(t)$, by integrating the local free hole flux (current density) over the domain and averaging, according to the equation

$$I(t) = A\frac{1}{n}\sum_{i=1}^{i=n} j_i = \frac{1}{n}A\mu_0\sum_{i=1}^{i=n}\exp\left(\gamma\sqrt{|E_i|}\right)\left(-k_B T\frac{\partial p_{f_i}}{\partial x} + p_{f_i}eE_i\right), \tag{4}$$

where A is the film cross-sectional area (contact area with the electrodes) and j is the current density. For simplicity, Eq. (4) assumes a uniform grid of n points (nodes 'i'); the subscripts i in the quantities of the right-hand sides of Eq. (4) denote the nodal values of the quantities.

3. Results and discussion

Before comparing the predictions of our model with the experimentally measured transient photocurrents in our P3HT samples, we validated the model by fitting its predictions to the experimental $I(t)$ data from the TOF measurements of Ref. [13] for nondispersive hole transport in the polyfluorene copolymer poly[(9,9-dioctylfluorenyl1-2,7-diyl)-co-(4,4′-(N-(4-sec-butylphenyl))diphenylamine)]. The model reproduced the data successfully throughout the duration of the TOF experiment, including the initial increase, plateau region, and tail region of the transient photocurrent [13]. Having validated the model, we solved the coupled BVPs governed by Eqs. (1)–(3) and fitted our experimental $I(t)$ measurements for our P3HT samples, thus obtaining as fitting parameters hole transport properties, kinetic coefficients, and material properties for the different nanostructured P3HT films used in the TOF experiments.

We modeled hole transport under various applied biases in a 4-μm-thick P3HT drop-cast thin film (sample P1), thin films of non-centrifuged nanoparticle assemblies with excess surfactant molecules of thickness equal to 0.5 μm (sample P2) and 1.5 μm (sample P3), and a 2.5-μm-thick film of centrifuged nanoparticle assemblies with the excess surfactant molecules removed (sample P4). We found that hole transport dynamics is significantly different in these films of different nanostructures. Figures 1(a)–(d) show the evolution of the free hole density profiles in these four samples under certain applied biases; in each figure, the inset depicts the evolution of the corresponding trapped hole density profile. It is evident that trapping and detrapping of charge carriers due to structural defects in the amorphous layer distort the charge density profile from a Gaussian distribution [17]. The peak locations of the free and trapped hole packets propagate in the polymeric materials of our samples at speeds determined by